Improved Antimicrobial Properties of Methylene Blue Attached to Silver Nanoparticles

Ermek Belekov[a], **Khomidkhodza Kholikov**[a], **Lauren Cooper**[a], **Simran Banga**[b], **Ali O. Er**[a]

[a]Western Kentucky University, Department of Physics and Astronomy, Bowling Green, KY 42101

[b]Western Kentucky University, Department of Biology, Bowling Green, KY 42101

Abstract

Photosensitizing agents are the cornerstone of Photodynamic Therapy (PDT) that play essential role in deactivation process of multidrug resistant pathogens and tumor treatments. In this work, we studied a photosensitizing agent made from mixture of Silver Nanoparticles (Ag NPs) and Methylene Blue (MB) which possess improved important characteristics like high photostability and high singlet oxygen yield. Ag NPs were synthesized by pulsed laser ablation technique in different aqueous solutions like polyvinylpyrrolidone (PVP), citrate and Deionized (DI) water. The synthesized AgNPs were characterized in depth using with transmission electron microscopy (TEM), UV-Visible (UV-Vis), and photoluminescence (PL) spectra. These Ag NPs were combined with MB and used to eradicate the Gram-negative bacteria, *Escherichia coli (E. coli)*, and Gram-positive bacteria, *Staphylococcus aureus (S. aureus)*. MB and Ag NPs mixture was found to possess higher antimicrobial activity and thus were more effective in killing both Gram – positive and Gram-negative bacteria in comparison to individual exposure of MB and Ag NPs. Additionally, the antimicrobial effects varied with respect to the size of nanoparticles as well as the medium used for their synthesis. The data from this study supports the potential use of the proposed method in PDT where standard photosensitizers have limitations.

Keywords

silver nanoparticles; methylene blue; bacteria deactivation; photodynamic therapy

Introduction

Bacterial infections are a major cause of chronic infections and lead to high mortality of humans and animals. One of the major treatment method commonly used for bacterial infections are antibiotics. However, the widespread use of antibiotics resulted in the emergence of multidrug-resistant or pathogenic bacterial strains. Consequently, the needs for developing new bactericidal materials and techniques gained importance. Photodynamic therapy (PDT) is proposed as an alternative method to eliminate multi-drug resistant

pathogens, malignant cells, and other diseased cells [1–3]. To make antimicrobial PDT more effective, along with a light source of the appropriate wavelength in the presence of tissue oxygen, an efficient photosensitizer is required. An ideal photosensitizer must possess strong absorbance at long wavelengths, excellent photostability, lower dark toxicity, and high quantum yield of singlet oxygen ($^1O_2$) [4, 5]. One of such photosensitizers is methylene blue (MB), that contains amazing photophysical and photochemical properties [6, 7]. By virtues of these properties, MB is used to control bacterial infection for skin treatment, dental therapy, and has shown promising results in *in vivo* regression of cancer and bacterial infections [7–10]. Under the irradiation of red (630–680 nm) light, MB is able to generate copious singlet oxygen, $^1O_2$, reactive oxygen species (ROS), and OH. It has been demonstrated that the photogenerated $^1O_2$ and ROS, reacts against tryptophan and the other outer-membrane molecules thereby damaging the bacterial cell and inhibiting protein production [9]. Nevertheless, the photodeactivation rate of MB was found to be significantly lower in plasma than in water, saline, and PBS solution; making it ineffective bacterial killing agent, especially in the human plasma [11]. However, MB attached to various carriers, including nanomaterials and quantum dots, enhanced their water solubility, improved their delivery into cancer cells, and showed synergistic effects in bacterial deactivation process [9, 12–14].

Silver nanoparticles (Ag NPs) is one of the most promising antimicrobial agent since they possess high germicidal activity against a broad range of microbes [15–17]. Moreover, the cost-effectiveness, availability as well as the lower toxicity toward human blood has attracted considerable attention of silver nanoparticles in the treatment of infectious diseases [18]. Disinfection with silver is well known wound management technique from ancient times. Silver has been used extensively for medical purposes since as early as 4,000 B.C.E. Persians, for instance, used silver jugs to keep water fresh especially during the military conflict when the fresh water was not readily available [19]. Later, records shows that silver has been used as a blood purifier, counterirritant, even in the treatment of brain infections [19]. A comprehensive research on the antibacterial action of Ag NPs started around 2004 with the advancement of nanotechnology, and rose exponentially since then [20, 21]. The possible mechanisms and bactericidal activity of Ag NPs have been discussed in many literature reviews, where the major causes underling the antibacterial effects of Ag NPs were explained as follows: 1) direct damage of bacterial cell membrane; 2) generation of reactive oxygen species by silver nanoparticles and silver ions; 3) penetration of NPs into the bacterial cell membrane; and 4) induction of intracellular antibacterial effects, including disruption of Adenosine triphosphate (ATP) production and DNA replication [22–24]. The most critical physical and chemical parameters that affect the antimicrobial potential of Ag NPs are size, shape, surface charge, concentration and colloidal state [25–27].

Ag NPs have been synthesized by many different methods to date [28]. Among these methods, Liquid Phase Pulsed Laser Ablation (LP-PLA) technique offers a green, inexpensive, and fast route to Ag NPs synthesis. In addition, by LP-PLA method the composition of the NPs can be easily controlled by varying the aqueous ablation liquid and the laser parameters [29]. Some studies have shown the influence of adducts such as surfactants and volume-excluders on the size, monodispersity, and stability of nanoparticles. For instance, the addition of a proper amount of NaCl reduced the particles size distribution

[30]; the synthesized NPs' size was decreased with increased concentration of sodium dodecyl sulfate (SDS); polyvinylpyrrolidone (PVP) aqueous solution improved obtained colloid's stability as well as decreased the average size of NPs [31].

In this work, we have synthesized Ag NPs in citrate, PVP aqueous solutions, and in DI water by using LP-PLA method. Ag NPs were characterized by FTIR, UV-Vis spectroscopy, and PL spectra. NP size distribution quantification was performed by transmission electron microscopy (TEM) images. Later, these synthesized Ag NPs in different aqueous solution along with commercial Ag NPs at 10 nm, 20 nm, and 40 nm size distributions was mixed with MB to increase singlet oxygen generation and photoresponsivity. In our study, we found Ag/MB mixture was more effective antibacterial compared to MB, and Ag nanoparticles alone. MB/Ag coupled with 5 minutes of irradiation at 660 nm light, eliminated all Gram–negative and –positive bacteria colonies. Moreover, in this study we explored the influence of the size of NPs as well as the medium on its photodeactivation when mixed with MB.

Experimental

Ag NPs synthesis:

Ag NPs were synthesized in different aqueous solutions by targeting 1064 nm Nd: YAG laser beam (Continuum Surelite II, 10 Hz repetition rate, and 5 ns pulse duration) to the silver surface as illustrated in Fig. 1. The silver target (99.99%, thickness 1.0 mm, Sigma-Aldrich) was adhered to the bottom of 500 ml beaker with double-sided carbon tape. Then 60 ml of ablation liquid was added to the beaker thereby making the liquid height above the target 11 mm.

After, the beaker was placed on the XY-translation stage to control the position of laser beam relative to the target. In addition, this setup was rotated by shaker at 312 rpm to prevent accumulation of Ag NPs above the target and to minimize shielding effects. The laser beam was focused by converging lens with 300 mm focal length, and its power was set up to 200–220 mJ. The ablation time took 10–15 minutes.

Characterization techniques:

The morphology, microstructure and the average size distribution of synthesized Ag NPs were analyzed with TEM images placing a droplet onto a 300-mesh copper TEM grid. UV-vis spectrophotometer was used to study the absorbance of Ag NPs in different aqueous medium, and to measure the singlet oxygen generations of MB, Ag NP, and Ag/MB by record the optical density rate of 9, 10- anthracenediyl-bis (methylene) dimalonic acid (ABMDMA) at 400nm. Finally, the photoluminescence spectra (PL) of Ag NPs in various solutions acquired by spectrofluorometer.

Bacterial culture experiment:

The antibacterial activity of synthesized Ag NPs, MB, and the Ag-MB combination were evaluated by using the *S. aureus* and *E. coli* bacteria. Bacteria were cultured in LB broth media by incubating for 24–48 hrs. Subsequently, 10^6 colony forming units/ml concentration

of bacteria were inoculated to 8 different disposable plates as shown in Fig 2. Here 4 different sample groups were prepared in duplicate which comprised of (1) bacteria only, (2) bacteria + Ag NPs, (3) bacteria + MB, (4) bacteria + MB-Ag plates. The actual experimental setup can be seen in Fig. 2c. One of the sample from each group were exposed with red LED for 3–5 minutes, while the other one were kept as a control. The bacterial counts of each sample were obtained in duplicate after 24 hours incubation at 37 °C.

Results and Discussions

We have used both commercially available nanoparticles (Citrate, NanoXact) and samples prepared with pulsed laser synthesis method as described above. Different characterization methods have been used to understand the morphology and physical and chemical properties of the silver nanoparticles.

TEM measurements

The shape and the particles size distribution were studied by transmitting electron microscopy (TEM) images. Figure 3 illustrates the TEM images of Ag NPs in citrate solution and DI water. Our statistical analysis show that the distribution is Gaussian with mean average of 10 nm, 20nm, and 48nm for commercial samples (10 nm, 20nm, 40 nm Silver Nanospheres, Citrate, NanoXact).

The average size distribution of our synthesized Ag NPs were found as follows: in DI water 23 nm; in citrate (Sodium Citrate Dihydrate, Fisher) aqueous solution with concentration of 2mM was found to be 10 nm; in 2mM Polyvinylpyrrolidone (PVP, Sigma-Aldrich) aqueous medium the average size distribution was 15 nm. The TEM results show large distance between individual nanoparticles. Therefore, it can be concluded that electronic coupling between nanoparticles is negligible and doesn't contribute their optical spectra. However, it should be noted that aggregation, as observed in Fig. 3c and 3d, occurs when weak physical forces bring particle surface in contact with each other and short range thermodynamic interactions results in particle attachment. This is especially true for particle whose size is less than 100 nm where Brownian motion controls the long-range forces [32].

Uv-Vis Spectrum:

It is known that small nanoparticles shows distinct properties such as absorption and scattering compared to bulk materials. Collective coherent excitations of free electros in the conduction of the nanoparticles, also known as surface plasmonics resonance, leading to enhanced local electric field, are responsible for the strong absorption and scattering.

The UV-Vis spectrum absorption peaks for Ag NPs in citrate, PVP, and DI water solutions right after 10 minutes of irradiation with 210 mJ/pulse pulsed laser were determined at 392 nm, 397 nm, and 399 nm respectively as shown in Fig. 4 (a). These peak distinctions occurred due to size distribution difference as the diameter of NPs increases the peak of plasmon resonance shifts to longer wavelengths and broadens.

Smaller nanospheres primarily absorb light and have peaks near 400 nm, while larger spheres exhibit increased scattering and have peaks that broaden and shift towards longer wavelengths (known as red-shifting) [33, 34].

Our TEM analysis also shows that the average size distribution of Ag NPs obtained in citrate medium is much smaller than in PVP solution or in DI water; 10 nm (UV-Vis peak: 392nm) vs 15 nm (UV-Vis peak: 397nm) and 23 nm (UV-Vis peak: 399nm) respectively. The size of NPs obtained through LP-PLA technique depends on thermodynamic properties of plasma such as temperature, pressure, and density of aqueous solution [31, 35, 36]. It has been reported that the increased density and viscosity of solvents by PVP also increases the plasma confinement during the ablation process [31]. In addition, pressure inside the cavitation bubble in PVP (or citrate) solution is higher than in DI water, which in turn results in decreased sizes of ablated NPs [31].

In addition, plasma species inside PVP solution were found to be more confined by the solvent compared to water. This increased plasma confinement is probably due to higher density and viscosity of the PVP.

Figure 4 (b) shows how the UV-Vis absorbance peaks shift for each medium over time. This spectroscopy provides stability analysis, since in case of multi-nanoparticle aggregate the plasmon resonance will be shifted to a longer wavelength. We found the Ag NPs in DI water is relatively stable. Moreover, it can be observed that Ag NPs in citrate medium after rapid changes in first 4 weeks become more stable, while the absorbance peak of Ag NPs in PVP solutions continuously changes showing the accumulation of NPs to bigger colloids. It should be noted that although initial electronic coupling is negligible, the nanoparticles in the containers interact with each other electronically, causing aggregation and leading to the shift in the spectra.

Photoluminescence (PL) Measurements

The photoluminescent emission spectroscopy was employed to study the optical properties of Ag NPs. Figure 6 shows the excitation dependent photoluminescence of Ag NPs in citrate, PVP, and DI water solutions.

The silver nanoparticles show size-dependent photoluminescence emission due to SPR. The strong SPR will eventually lead to enhancement of the quantum yield of the photoluminescence [37–39]. The peak absorption wavelength and width of the absorption band depends on the size, shape, spatial orientation, and optical properties of the nanoparticles and solvent medium.

It was shown that maximum PL band was close to interband absorption edge, possibly due to interband radiative transitions. In addition, as our results show in Fig. 7a, when the size of the silver nanoparticles decreases, the intensity of the PL increases. This indicates a strong influence of nanoparticle surface on the PL spectra. It should be noted that when the size of the particles becomes smaller than the mean-free path of the electrons in bulk metal, the electron-surface scattering of the particles leads to the broadening of the SPR band and is referred as the internal size effect [40]. The radiative damping effect causes the decrease in

the local electric field inside the particles when the silver nanoparticles size become 40 nm. Eventually, this leads to a decrease in P intensity as shown in Fig. 6a. Furthermore, in figure 6 the PL emissions at 310 nm excitation light for Ag NPs are compared according to their size distribution and the medium.

Singlet oxygen measurement:

From photo-degradation of ABMDMA in MB, Ag NPs, and MB/Ag NPs solutions over irradiation time, the singlet oxygen generation have been determined. Here, we compared the amount of singlet oxygen generation according to the size and the aqueous medium of nanoparticles (Fig. 7). The slopes of Ag NPs alone independently from size and medium were zero, which ascertains no ROS yield. However, the combination of Ag NPs with MB surpassed the $^1O_2$ generation of MB alone.

This can be due to contribution of nanoparticles to increase the lifetime of the triplet state of MB, or improvement of intersystem crossing (ISC) [41–43]. It is also important to note that as the size of Ag NPs decreases the ROS production increases, which may be due to higher interaction of small sized Ag NPs with MB because of the greater surface area to volume ratio. Finally, the singlet oxygen generation in DI water was higher than in PVP and citrate solution.

pH Measurements:

Microbial growth is significantly influenced by environmental conditions such as temperature, pH, oxygen levels, micronutrient and salt concentrations [44, 45] (1, 2). In laboratory, these environmental factors can be standardized with the use of a specific growth media and incubation parameters. In order to assess the effect of different aqueous solutions used in the synthesis of Ag NPs on bacterial growth, we measured the pH of different silver nanoparticles (Table 1). The pH of Ag NPs varied from 6.0 to 8.5 depending on the aqueous solution used in the synthesis process. This pH variation didn't have any major effect on the growth of E.coli, however it marginally affected the growth of S. aureus in the absence of MB (Fig 8 & 9) during photodeactivation. Various studies have shown that optimal pH for bacterial growth is 6.8 to 7.4 and changes in pH can impact bacterial counts [46–48].

Bacteria experiment results:

Our results show that the Ag/MB combination can entirely deactivate 10^6 CFU/ml Gram-negative *E. coli* and Gram positive *S. aureus* bacteria in 5 minutes of irradiation time. Initially, bacteria samples with silver nanoparticles without any light treatment hasn't showed any decreased the in number of colonies. The results showing the effects of Ag NPs size distribution, and Ag/MB combination toward *E.coli* and *S. aureus* bacteria after 3 minutes of irradiation is seen in Fig.8. Ag/MB combination showed higher bactericidal effects than MB and Ag NPs alone for both E.coli and S.aureus bacteria. The synergistic effect of $AgNO_3$ and MB mixture against five different bacterial strains including *Serratia marcescens* and *E.coli has been previously demonstrated by Li et al.* [9]. In this study we report improved germicidal activity of MB coupled with Ag NPs in PDT, under different conditions. In addition we explored two different parameters that influence the germicidal activity. Firstly, we observed the influence of size of Ag NPs on inhibition of bacteria when

mixed with MB. Secondly, we have showed how the Ag NP's synthesized medium as well as the combination of MB and Ag NPs on that medium affects deactivation process. Our results suggest that as the size of Ag NPs decreases, it becomes more toxic toward both Gram-negative and Gram-positive bacteria (Fig.8). This can be due to higher probabilities of small Ag NPs to penetrate into bacteria, and damage DNA and mitochondria[49, 50]. Moreover, as particle size decreases the surface area-to-volume ratio increases, which leads to higher accumulation of Ag NPs to the bacterial surface; blocking the respiratory system and making it more toxic especially for an aerobic bacteria[51, 52]. In the presence of MB:Ag NPs, the number of bacterial colony forming units significantly dropped compared to the samples treated with MB only and Ag NPs, within 3 minutes of irradiation time. The cellular morphology alteration and membrane disruption caused by Ag NPs may create permeable holes for MB, which after entering the cell generates singlet oxygen and cause bacterial inactivation. It is important to note, the red light itself has no effect on bacteria viability as well as MB in the absence of light [13].

Our data showed a higher sensitivity of *E. coli* than *S. aureus* when MB mixed with Ag NPs. Interestingly, Ag NPs only solution shows partial suppression of S. aureus but not E. coli which can be due to the peptidoglycan concentration differences between the two strains[27].

We also tested how the nanoparticle synthesizing medium affects the viability of bacterial strains after PDT treatment. The results after 3 minutes of irradiation suggest that Ag NPs in DI water are more effective in eradication process compared to PVP and citrate solutions as shown in Figure 9. This might be due to higher release of silver ions (Ag^+) in water enabling Ag^+ to interact with a number of electron donor functional group such as thiols, phosphates, hydroxyls, imidazole, and indoles[23, 50]. For instance, once interacts with the thiol group of the mitochondrial membrane protein, it causes the mitochondrial dysfunction and hence disrupts the cell's energy production [53]. Moreover, developed electrostatic force between negatively charged bacterial cells and positively charged nanoparticles promotes higher interaction between the two entities [54, 55].

Conclusion

Ag NPs with average size distribution of 23 nm in DI water, 8.43 nm in citrate solution, and 20 nm in PVP medium were synthesized by LP-PLA method. Material characterizations of Ag NPs were performed by UV-Vis, PL and EDS spectroscopy, while the size distribution and the shape of Ag NPs were studied with TEM images. MB/Ag NPs combination increased the singlet oxygen generation as well as showed higher antimicrobial effects compared to MB and Ag NPs alone. Within 5 minutes of irradiation time with 660nm LED, the MB/Ag NPs deactivated entire ~ 10^6 CFU/ml concentrated Gram-positive, *S.aureus*, and Gram-negative, E.coli, bacteria. MB/Ag NPs used in PDT could be effective in killing bacterial pathogens in open wounds, prosthetic joint infections, *in vivo* cancer and tumor treatments.

Acknowledgements

References

[1]. Bulina ME, Chudakov DM, Britanova OV, Yanushevich YG, Staroverov DB, Chepurnykh TV, Merzlyak EM, Shkrob MA, Lukyanov S, and Lukyanov KA, Nat Biotechnol 24 (2006) 95. [PubMed: 16369538]

[2]. Habiba K, Encarnacion-Rosado J, Garcia-Pabon K, Villalobos-Santos JC, Makarov VI, Avalos JA, Weiner BR, and Morell G, Int J Nanomedicine 11 (2015) 107. [PubMed: 26766909]

[3]. Hamblin MR and Hasan T, Photochem Photobiol Sci 3 (2004) 436. [PubMed: 15122361]

[4]. Briggs T, Blunn G, Hislop S, Ramalhete R, Bagley C, McKenna D, and Coathup M, Lasers Med Sci 33 (2018) 523. [PubMed: 29247432]

[5]. Fu X, Fang Y, and Yao M, Biomed Res Int. 2013 (2013) 159157. doi 10.1155/2013/159157. Epub 2013 Feb 28. [PubMed: 23555074]

[6]. Severino D, Junqueira HC, Gugliotti M, Gabrielli DS, and Baptista MS, Photochem Photobiol 77 (2003) 459. [PubMed: 12812286]

[7]. Wojtoniszak M, Rogi ska D, Machali ski B, Drozdzik M, and Mijowska E, Materials Research Bulletin 48 (2013) 2636.

[8]. Dai T, Huang Y-Y, and Hamblin MR, Photodiagnosis and Photodynamic Therapy 6 (2009) 170. [PubMed: 19932449]

[9]. Li R, Chen J, Cesario TC, Wang X, Yuan JS, and Rentzepis PM, Proceedings of the National Academy of Sciences 113 (2016) 13612.

[10]. Zeina B, Greenman J, Purcell WM, and Das B, Br J Dermatol 144 (2001) 274. [PubMed: 11251558]

[11]. Er AO, Chen J, Cesario TC, and Rentzepis PM, Photochem Photobiol Sci 11 (2012) 1700. [PubMed: 22833174]

[12]. Chatterjee DK, Fong LS, and Zhang Y, Adv Drug Deliv Rev 60 (2008) 1627. [PubMed: 18930086]

[13]. Kholikov K, Ilhom S, Sajjad M, Smith ME, Monroe JD, San O, and Er AO, Photodiagnosis Photodyn Ther 24 (2018) 7. [PubMed: 30144532]

[14]. Yoon HK, Ray A, Lee YE, Kim G, Wang X, and Kopelman R, J Mater Chem B 1 (2013)

[15]. Lara HH, Garza-Trevino EN, Ixtepan-Turrent L, and Singh DK, J Nanobiotechnology 9 (2011) 1477.

[16]. Rai M, Yadav A, and Gade A, Biotechnol Adv 27 (2009) 76. [PubMed: 18854209]

[17]. Rai MK, Deshmukh SD, Ingle AP, and Gade AK, J Appl Microbiol 112 (2012) 841. [PubMed: 22324439]

[18]. Dakal TC, Kumar A, Majumdar RS, and Yadav V, Front Microbiol 7 (2016)

[19]. Alexander JW, Surg Infect 10 (2009) 289.

[20]. Le Ouay B. and Stellacci F, Nano Today 10 (2015) 339.

[21]. Sondi I. and Salopek-Sondi B, J Colloid Interface Sci 275 (2004) 177. [PubMed: 15158396]

[22]. Duran N, Duran M, de Jesus MB, Seabra AB, Favaro WJ, and Nakazato G, Nanomedicine 12 (2016) 789. [PubMed: 26724539]

[23]. Franci G, Falanga A, Galdiero S, Palomba L, Rai M, Morelli G, and Galdiero M, Molecules 20 (2015) 8856. [PubMed: 25993417]

[24]. Wang L, Hu C, and Shao L, Int J Nanomedicine 12 (2017) 1227. [PubMed: 28243086]

[25]. Helmlinger J, Sengstock C, Groß-Heitfeld C, Mayer C, Schildhauer TA, Köller M, and Epple M, RSC Advances 6 (2016) 18490.

[26]. Ivask A, Kurvet I, Kasemets K, Blinova I, Aruoja V, Suppi S, Vija H, Käkinen A, Titma T, Heinlaan M, Visnapuu M, Koller D, Kisand V, and Kahru A, PLOS ONE 9 (2014) e102108.

[27]. Kim TH, Kim M, Park HS, Shin US, Gong MS, and Kim HW, J Biomed Mater Res A 100 (2012) 1033. [PubMed: 22308013]

[28]. Tran QH, Nguyen VQ, and Le A-T, Advances in Natural Sciences: Nanoscience and Nanotechnology 4 (2013) 033001.

[29]. Au - Ratti M, Au - Naddeo JJ, Au - Griepenburg JC, Au - O'Malley SM, Au - Bubb DM, and Au - Klein EA, JoVE (2017) e55416.

[30]. Bae CH, Nam SH, and Park SM, Applied Surface Science 197–198 (2002) 628.

[31]. Tsuji T, Thang DH, Okazaki Y, Nakanishi M, Tsuboi Y, and Tsuji M, Applied Surface Science 254 (2008) 5224.

[32]. Barberio M. and Antici P, Scientific Reports 7 (2017) 41372. [PubMed: 28195194]

[33]. Huang X. and El-Sayed MA, Journal of Advanced Research 1 (2010) 13.

[34]. Fong KE and Yung L-YL, Nanoscale 5 (2013) 12043. [PubMed: 24166199]

[35]. Li Y, Musaev OR, Wrobel JM, and Kruger MB, Journal of Laser Applications 28 (2016) 022004.

[36]. Phuoc TX, Soong Y, and Chyu MK, Optics and Lasers in Engineering 45 (2007) 1099.

[37]. Yeshchenko OA, Dmitruk IM, Alexeenko AA, Losytskyy MY, Kotko AV, and Pinchuk AO, Physical Review B 79 (2009) 235438.

[38]. Bohren A. a. s. o. C. F. and Huffman DR and Y N. light by small particle Wiley, 1998,

[39]. O. P. o. M. C. U. Kreibig and M. Vollmer, Springer, Berlin, Heidelberg, 1995.

[40]. Olson J, Dominguez-Medina S, Hoggard A, Wang L-Y, Chang W-S, and Link S, Chemical Society Reviews 44 (2015) 40. [PubMed: 24979351]

[41]. Ge J, Lan M, Zhou B, Liu W, Guo L, Wang H, Jia Q, Niu G, Huang X, Zhou H, Meng X, Wang P, Lee CS, Zhang W, and Han X, Nat Commun 5 (2014)

[42]. Markovic ZM, Ristic BZ, Arsikin KM, Klisic DG, Harhaji-Trajkovic LM, Todorovic-Markovic BM, Kepic DP, Kravic-Stevovic TK, Jovanovic SP, Milenkovic MM, Milivojevic DD, Bumbasirevic VZ, Dramicanin MD, and Trajkovic VS, Biomaterials 33 (2012) 7084. [PubMed: 22795854]

[43]. Ristic BZ, Milenkovic MM, Dakic IR, Todorovic-Markovic BM, Milosavljevic MS, Budimir MD, Paunovic VG, Dramicanin MD, Markovic ZM, and Trajkovic VS, Biomaterials 35 (2014) 4428. [PubMed: 24612819]

[44]. Mil'ko ES, E. N. V. f.-k. f. s. n. r. d. n. g. n. b. T. e. o. p. e. f. o. t. g. o. g.-p. b..

[45]. Ichhpujani R, Bhatia R, & Ichhpujani R. (2008). Nutrition and Growth of Bacteria. In Essentials of Medical Microbiology (pp. 22–22). Jaypee Brothers Medical Publishers (P) Ltd. 10.5005/jp/books/10281_4,

[46]. Fabrega J, Fawcett SR, Renshaw JC, & Lead JR (2009). Silver nanoparticle impact on bacterial growth: Effect of pH, concentration, and organic matter. Environmental Science and Technology, 43(19), 7285–7290. 10.1021/es803259g, [PubMed: 19848135]

[47]. Rodriguez-Caturla MY, Valero Díaz A, Vallejo JLR, García-Gimeno RM, & Cosano GZ (2012). Effect of pre-incubation conditions on growth and survival of Staphylococcus aureus in sliced cooked chicken breast. Meat Science, 92(4), 409–416. 10.1016/j.meatsci.2012.05.003, [PubMed: 22658427]

[48]. Sánchez-Clemente R, Igeño MI, Población AG, Guijo MI, Merchán F, & Blasco R. (2018). Study of pH Changes in Media during Bacterial Growth of Several Environmental Strains. Proceedings, 2(20), 1297.,

[49]. Tamayo LA, Zapata PA, Vejar ND, Azocar MI, Gulppi MA, Zhou X, Thompson GE, Rabagliati FM, and Paez MA, Mater Sci Eng C Mater Biol Appl 40 (2014) 24. [PubMed: 24857461]

[50]. Wu D, Fan W, Kishen A, Gutmann JL, and Fan B, J Endod 40 (2014) 285. [PubMed: 24461420]

[51]. Matsumura Y, Yoshikata K, Kunisaki S, and Tsuchido T, Appl Environ Microbiol 69 (2003) 4278. [PubMed: 12839814]

[52]. Shrivastava S, Bera T, Roy A, Singh G, Ramachandrarao P, and Dash D, Nanotechnology 18 (2007) 225103.

[53]. Liao C, Li Y, and Tjong SC, International journal of molecular sciences 20 (2019) 449.

[54]. Guzman M, Dille J, and Godet S, Nanomedicine 8 (2012) 37. [PubMed: 21703988]

[55]. Hamouda T. and Baker JR Jr., J Appl Microbiol 89 (2000) 397. [PubMed: 11021571]

Highlights

- Silver nanoparticles (Ag NPs) in different mediums were obtained using nanosecond laser pulses

- Silver nanoparticles by SEM-EDS, FTIR, TEM, UV-Vis, photoluminescence spectra.

- Ag NPs sizes ranging from 10 to 40 nm were obtained.

- Ag NPs samples shows excitation dependent fluorescence and excellent photostability

- Methylene blue (MB) were used in combination with silver nanoparticles.

- MB-Ag NPs compound was shown to produce higher amount of singlet oxygen than MB alone

- Gram positive and negative bacteria solution containing MB-Ag NPs were irradiated with red light

- MB-Ag NPs was shown to be more effective method for pathogen deactivation than MB and Ag NPs alone and has potential to be used in open wounds and skin cancer and where antibiotic resistance is present.
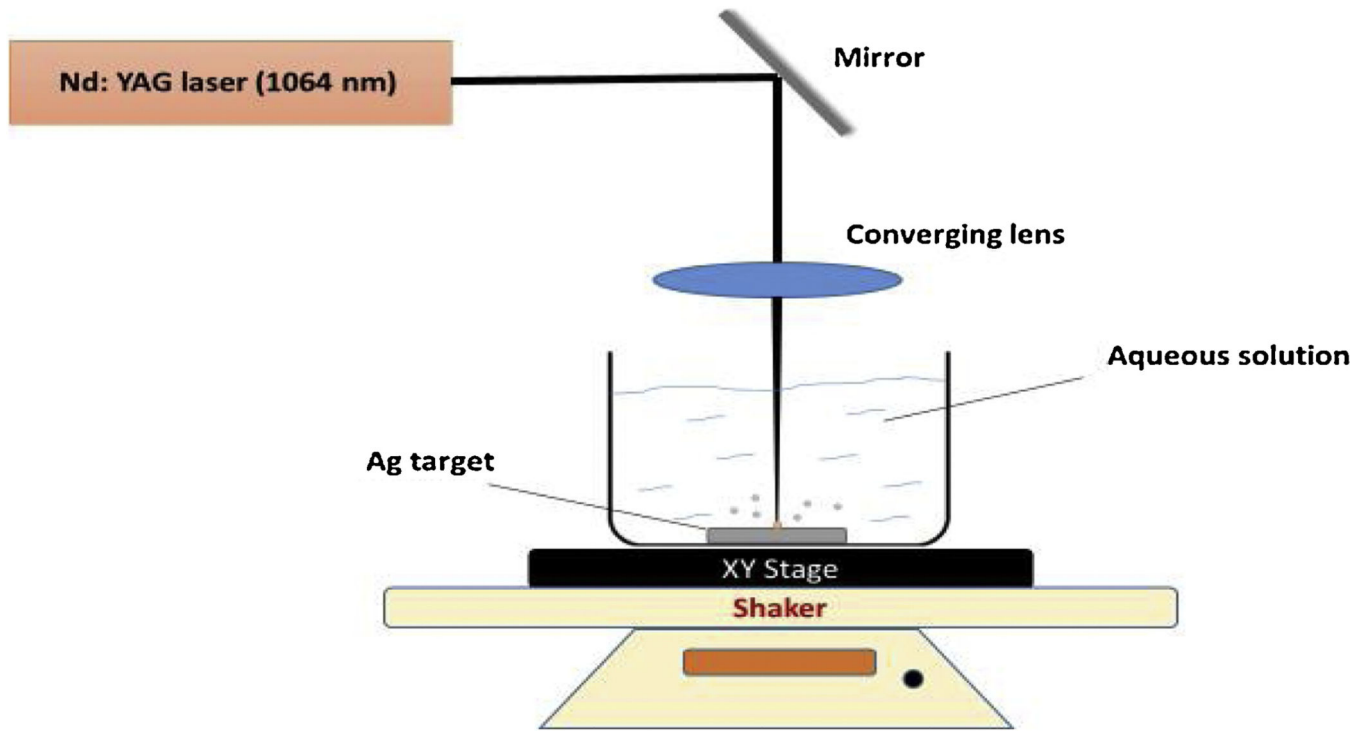
Figure 1.
Experimental setup for silver nanoparticle growth
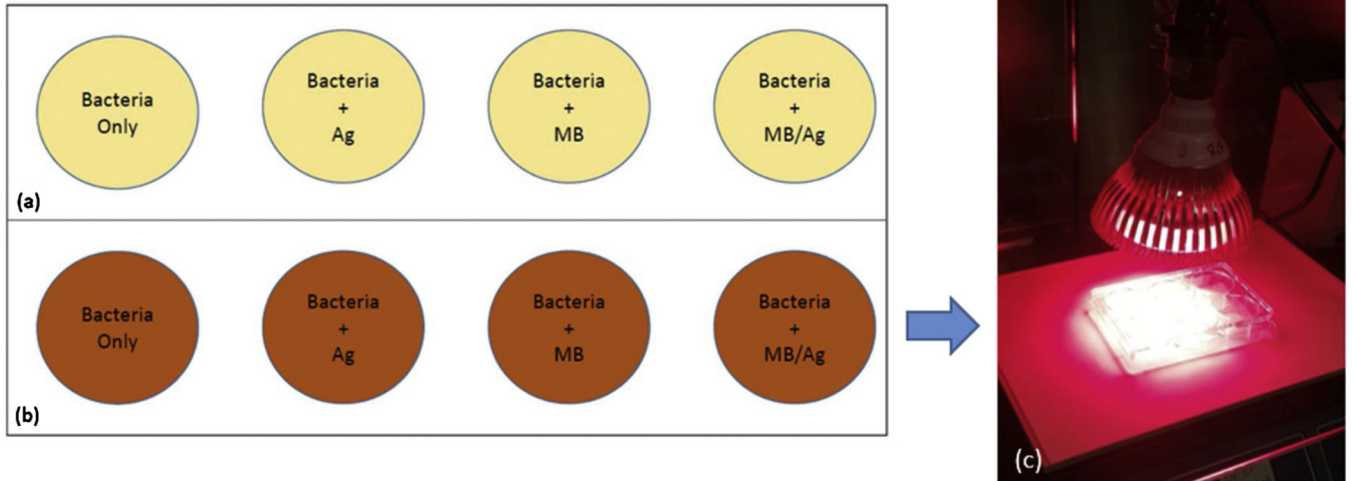
Figure 2.
a) Control samples b) Irradiated samples (c) actual experiment with 660 nm light
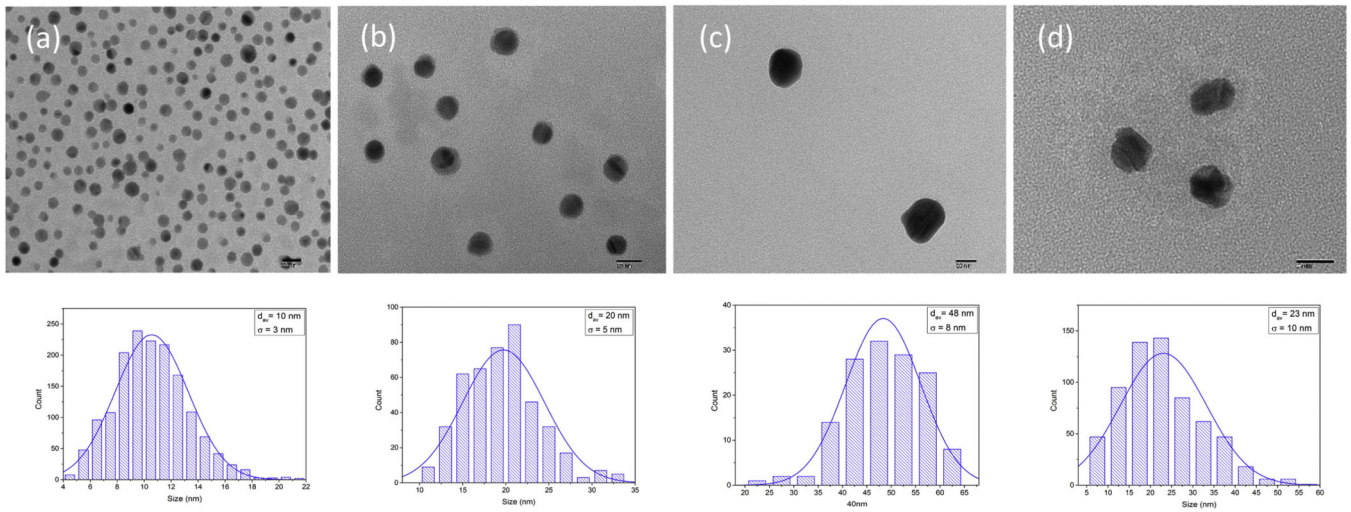
Figure 3.
Upper panel: TEM images of different size distributed Ag NPs in citrate solution (a) 10 nm average size (b) 20 nm average size (c) 48 nm average size (d) Ag NPs in DI water. Lower panel: The particle size distribution of Ag NPs.
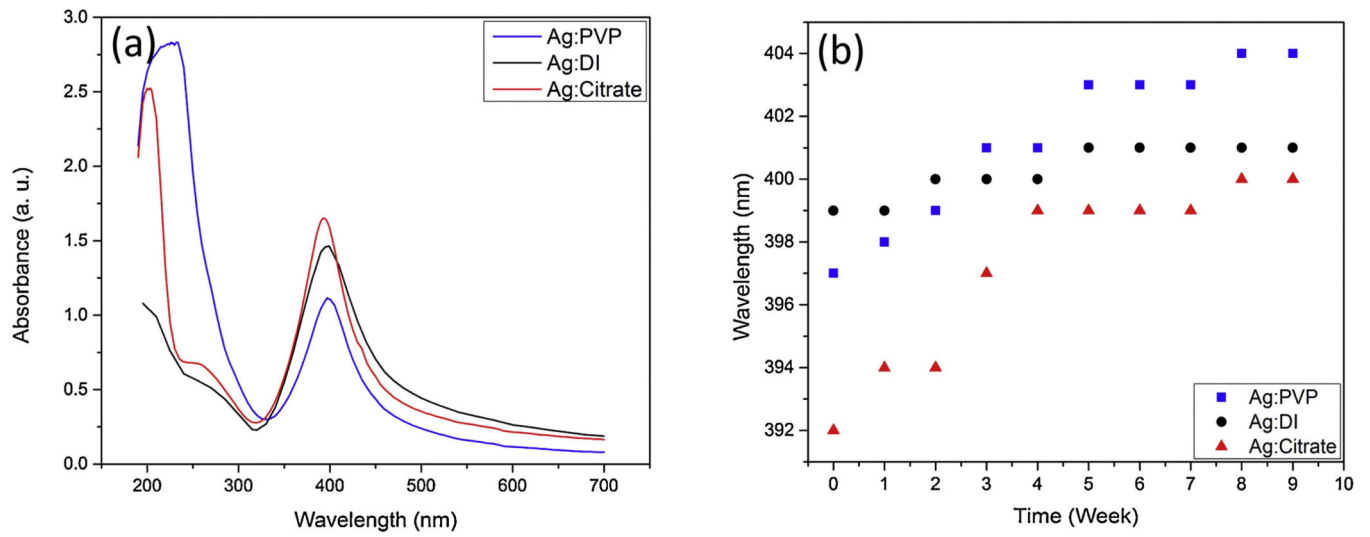
Figure 4.
(a) UV-Vis Spectrum of Ag NPs in PVP, DI and citrate solutions. (b) The changes of absorbance peak for each solutions over time.
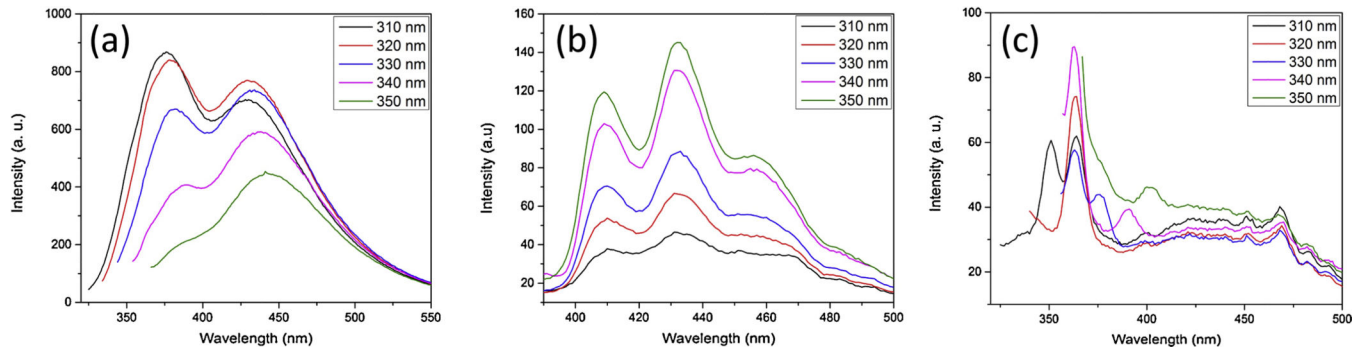
Figure 5.
(a) PL of Ag NPs in citrate solution (b) PL of Ag NPs in PVP solution (c) PL of Ag NPs in DI water
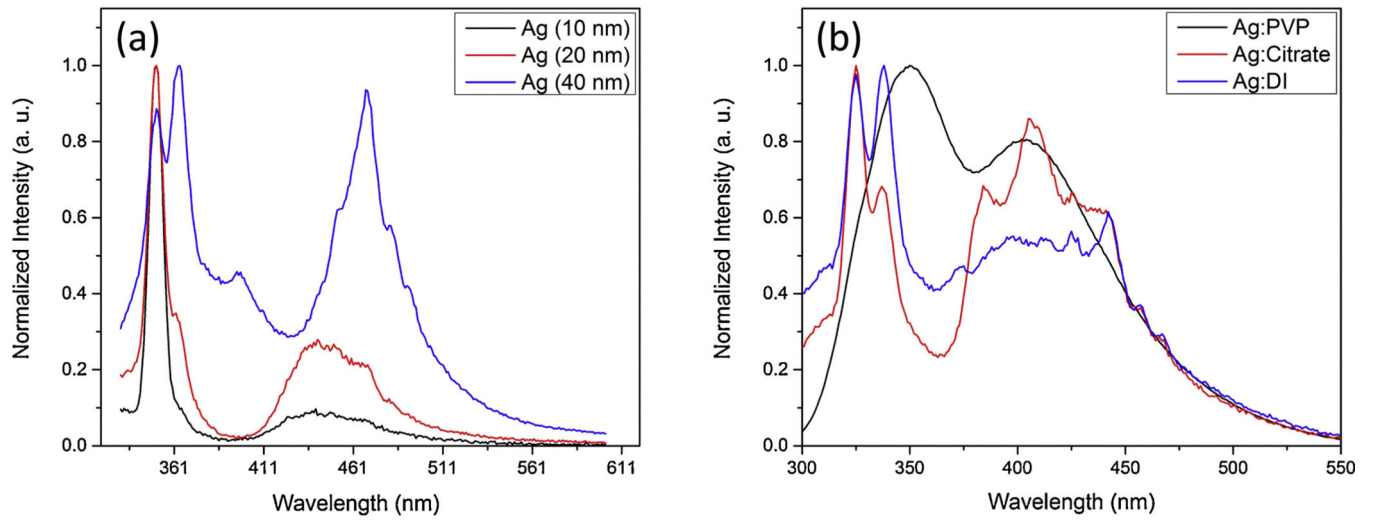
Figure 6.
(a) PL of Ag NPs in citrate solution with average size distribution of 10nm, 20nm, 40nm (b) PL of Ag NPs in PVP, citrate, and DI water.
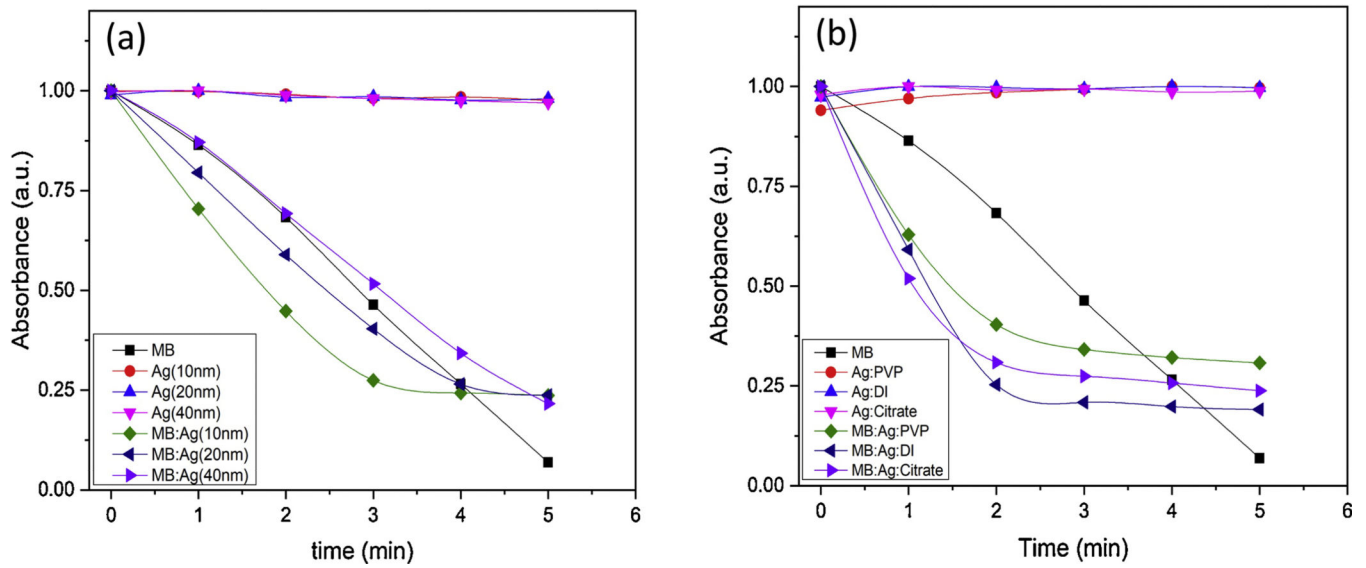
Figure 7.
Singlet oxygen generation of Ag NPs, MB, and Ag:MB at different time intervals. (a) For commercial 10, 20, and 40 nm Ag NPs. (b) For synthesized Ag NPs in DI water, citrate, and PVP solutions.
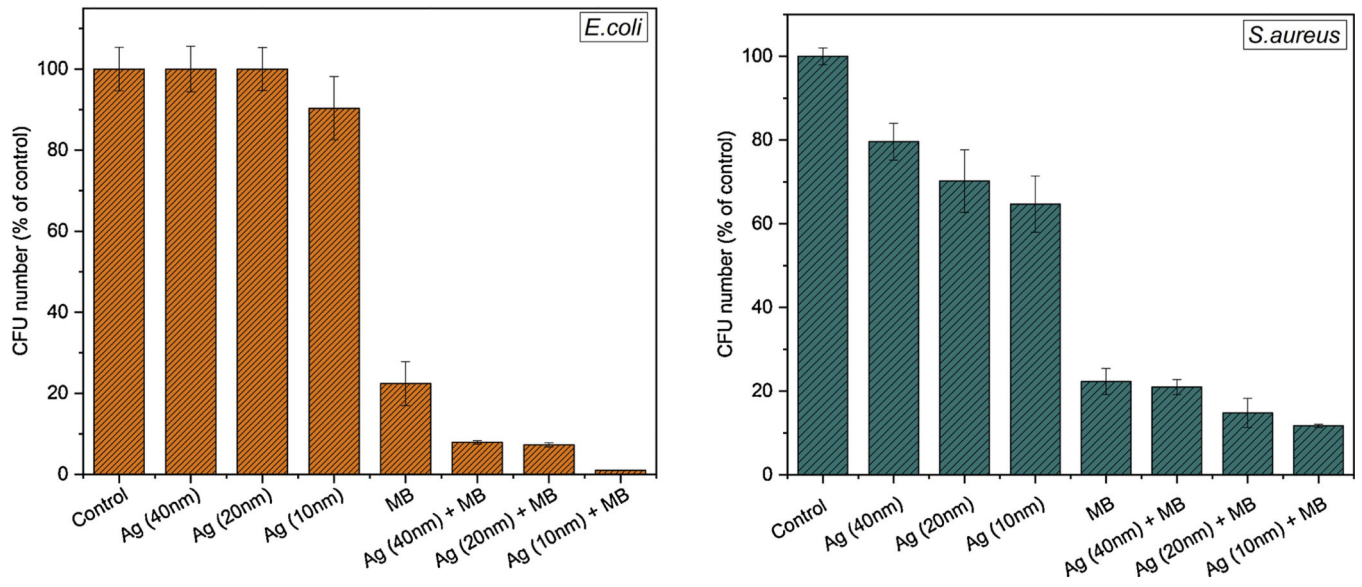
Figure 8.
E. coli (left) and S. aureus (right) bacteria CFU in percentages before and after 3 minutes irradiation with red (660nm) LED light.
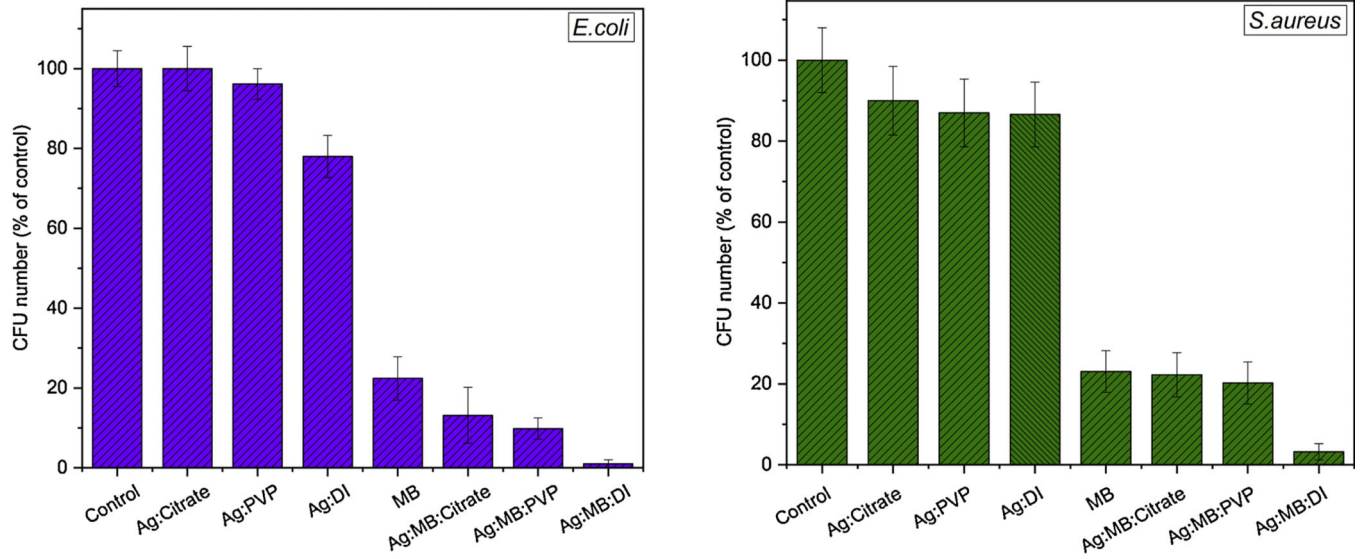
Figure 9.
E. coli (left) and S. aureus (right) bacteria CFU in percentages before and after 3 minutes
irradiation with red (660nm) LED light in different medium.

Table 1.

pH values of different medium

Substance	Citrate:Ag (10nm)	Citrate:Ag (20 nm)	Citrate:Ag (40nm)	PVP:Ag	DI:Ag	Citrate:Ag	PBS
pH	8.1	8.1	8.5	6.0	7.3	7.9	6.9